IMPROVED PARS-BASED PMRI IMAGE RECONSTRUCTION AS LINEAR APPROXIMATION

Yufang Bao

Department of Mathematics and Computer Science
Fayetteville State University, Fayetteville, NC 28304, USA

Abstract - *In this research, an improved approach to reconstruct high resolution brain images from Parallel Magnetic Resonance Imaging (pMRI) data is proposed based on the mathematical understanding that the PARS algorithms can be recast as linear approximates. It extends the PARS reconstruction method and is called IPARS in this paper. Our new improvements are in the following two aspects. First, localized significant coefficients of the Fourier series are selected and used for the reconstruction. Second, the maximum information from ACS lines have been retrieved and used for generating the coefficients for the reconstruction. The experiments have shown improved image reconstruction quality*.

Keywords: *pMRI, image reconstruction, IPARS algorithm, PARS algorithm, GRAPPA algorithm.*

1 Introduction

Acquisition of Magnetic Resonance Imaging (MRI) can be dramatically speeded up by using parallel imaging techniques, called Parallel MRI (pMRI), or Parallel Acquisition Technique (PAT). PMRI uses multiple receiver coils to simultaneously acquire several sets of *k*-space data with reduced samples in the phase encoding line direction. Fast imaging time is a critical factor in medical imaging, especially when we consider the inconvenience it might bring for patients. The imaging time can be dramatically reduced when the sampling rate is reduced to a level lower than the Nyquist sampling rate; however, the desired high resolution images can only be obtained in post-processing when an image reconstruction algorithm with a goal to achieve minimal compromise in the signal-to-noise ratio (SNR) is applied to all datasets and the sensitivity profile of all coils.

The development of an efficient image reconstruction algorithm is an important link in the successful implementation of pMRI technique. The direct result of subsampling is reduced field of view (FOV) in the reconstructed image with aliasing exhibited. In addition, a distinct inhomogeneous intensity across the imaging object is presented in images received from all coils due to each coil's reception sensitivity. All acquired datasets contain signals from the imaging object that have been modulated by the coil sensitivities, and can be described using a mathematical model to depict the Fourier transformation of signals from the spatial to the *k*-space domain. Such a model provides a theoretical framework for various parallel imaging reconstruction methods [1]. It has been used to reconstruct a high resolution image that clearly shows the imaging object that is free of sensitivity effects.

One reconstruction method for pMRI is in the spatial domain. The goal is to reproduce the exact full-resolution images that are sensitivity-invariant. This is represented by Generalized SENSE (GenSENSE), or SENSE (Sensitivity encoding), see [2,3,4]; both are referred to as SENSE-based algorithms. A typical problem with this type reconstruction is the under-determined problem due to an inverse matrix calculation, which is typically modified by regularizations, such as truncated SVD (Singular Value Decomposition) and Tikhonov regularization on matrix to obtain the Moore-Penrose pseudo inverse to alleviate this problem [5,6].

Another method of reconstruction is in the *k*-space domain. The goal is to directly reconstruct the sensitivity-invariant signals in full resolution. This is represented by a variety of SMASH and GRAPPA type algorithms, see [7-9]. In addition, research interest in the connection between the two category reconstruction methods has lead to further improvements on the reconstruction methods [10-21]. This research focuses on improving the PAR method that is further based on the GRAPPA algorithm.

The original GRAPPA algorithm [8] was developed as a two-step procedure. First, the under-sampled *k*-space data from each individual coil was interpolated to a full resolution version by a weighted combination of multiple lines and columns from data in neighboring coils. Second, the interpolated datasets from all coils are combined to obtain one synthesized full resolution *k*-space dataset that is sensitivity-invariant. The PARS method [10] improved the first step by interpolating the missing data from the combination of *k*-space data from neighboring coils that are located within an adaptive radius. These methods relax the strict requirements on the accuracy of the coil sensitivity maps, and they also reduce the burden of large computer

memory usage. However, problems, such as computational burden, and under-determined weights for the linear combination due to the limited coil spatial information, still persist in the GRAPPA-based algorithms. The problems became worsen with the increased number of weights to be determined.

In this paper, a new approach call IPARS algorithm is proposed based on the mathematical understanding that the GRAPPA-based algorithms can be recast as approximates, and based on the fact that the ACS lines can be viewed as being reconstructed from the sub-sampled data in its neighborhood, and vice versa. The experiments with our improved IPAR algorithm have shown improved image reconstruction quality.

2 Imaging Model

In this paper, the Cartesian system is considered and the volumetric MRI data acquired using multiple RF receiver coils can be described as:

$$S_l(k_x, k_y, k_z) = \sum_{x=0}^{N_x-1}\sum_{y=0}^{N_y-1}\sum_{z=0}^{N_z-1} r(x,y,z)c_l(x,y,z)e^{-j2\pi(xk_x+yk_y+zk_z)},$$

$$\text{for } l = 1,2,\cdots,L, \qquad (2.1)$$

where $r(x,y,z)$ is the spatial resonance signal (the sensitivity-invariant signal) that represents the density of an image object at (x,y,z). For the l-th coil, $l=1,\cdots,L$, $c_l(x,y,z)$ is the complex-valued spatial sensitivity map. $s_l(k_x,k_y,k_z)$ is the sensitivity modulated k-space data being subsampled with size of K_x, K_y, K_z, $K_x \le N_x, K_y \le N_y, K_z \le N_z$, where N_x, N_y, N_z is the size of the full resolution data in the k-space domain. Here (k_x, k_y, k_z), $k_x = 0,\cdots,K_x-1$, $k_y = 0,\cdots,K_y-1$, $k_z = 0,\cdots,K_z-1$ is referred to the sampling locations, in comparison, $(\omega_x, \omega_y, \omega_z)$ is usually referred to the location in the full resolution k-space. In this paper, a uniform sub-sampling scheme is referred, though an arbitrary sub-sampling scheme can be likewise described. The ratio of the amount of the fully acquired data compared to that of subsamples collected is defined as folds or reduction factors, M. The observed data from the l-th coil, $l=1,\cdots,L$, $d_l(k_x,k_y,k_z)$, can be described as

$$d_l(k_x,k_y,k_z) = s_l(k_x,k_y,k_z) + n_l(k_x,k_y,k_z) \qquad (2.2)$$

with noise $n_l(k_x,k_y,k_z)$ usually assumed as a Gaussian noise with independent identical distribution (i.i.d.) for each location.

For the sake of simplicity and to focus on discussing the relationship between the parallel imaging reconstruction methods, a single slice ($N_z = 1$) data will be used in Eqn. (2.1) though the formalism can be applied to volumetric data. Further, the noise term will be ignored in the following section; thus the data s_l is the same as d_l. Additionally, the subsampling is constrained to phase encoding (y direction) since regularized subsampling in the frequency encoding, or readout, direction will have no effect on the acquisition time [13].

3 The Extended GRAPPA Algorithm

In this section, an extended GRAPPA algorithm is connected to the GenSENSE through a best fit reconstruction using a mathematical model [23]. The characteristic of the GRAPPA style algorithms is that data of imaging object for each coil is reconstructed and combined to obtain a high resolution MR image of the object that is invariant to the sensor locations. The extended GRAPPA is indeed equivalent to the GenSENSE algorithm. To focus on the discussion of the extended GRAPPA and to simplify, $c_l(x,y) \neq 0$, $l = 1,\cdots,M$ are assumed when the extended GRAPPA reconstruction is derived, and we rewrite Eqn. (2.1) as

$$d_l(k_x,k_y) = \sum_{x=0}^{N_x-1}\sum_{y=0}^{N_y-1} r(x,y)c_{l'}(x,y)\frac{c_l(x,y)}{c_{l'}(x,y)}e^{-j2\pi(xk_x+yk_y)}, \quad l \neq l' \qquad (3.1)$$

By using the convolution theorem, the following equation can be obtained,

$$d_l(k_x,k_y) = \sum_{\omega_x}\sum_{\omega_y} d_{l'}(\omega_x,\omega_y)\tilde{c}_{l,l'}(k_x-\omega_x, k_y-\omega_y), \qquad (3.2)$$

where $c_{l,l'}(x,y) = \dfrac{c_l(x,y)}{c_{l'}(x,y)}$. Therefore, $\tilde{c}_{l,l'}(k_x,k_y)$ is the Fourier transformation of the ratio of sensitivities of two coils, i.e., the l-th and the l'-th coils. Thus the LHS, $d_l(k_x,k_y)$ in Eqn. (3.2) is the observed sub-sampled

k-space data from *l*-th coil, while $d_l(\varpi_x, \varpi_y)$ in the RHS of Eqn. (3.2) is the full resolution *k*-space data from the l'-th coil. This modified formula establishes a connection between the data from two different coils. It can be interpreted as an application of generalized series [21] where the l'-th coil data is served as the reference data for the data from the l-th coil.

A matrix $D_l = \tilde{C}_{l,l'} D_{l'}$ can be formed from Eqn. (3.2) and it leads to a large matrix system by integrating data from all coils $l \neq l'$ (the number of coils involved in the matrix is denoted as L', $L' \leq L$), therefore, we have

$$\begin{bmatrix} D_{l_1} \\ D_{l_2} \\ \vdots \\ D_{l_{L'}} \end{bmatrix} = \begin{bmatrix} \tilde{C}_{l_1,l'} \\ \tilde{C}_{l_2,l'} \\ \vdots \\ \tilde{C}_{l_{L'},l'} \end{bmatrix} D_{l'} \tag{3.3}$$

The full resolution *k*-space data, $D_{l'}$, of the l'-th coil can then be reconstructed as

$$D_{l'} = \sum_{l \neq l'} \left(\sum_{l'' \neq l'} \tilde{C}^H_{l'',l'} \tilde{C}_{l'',l'} \right)^{-1} \tilde{C}^H_{l,l'} D_l = \sum_l \hat{\tilde{C}}_{l,l'} D_l \tag{3.4}$$

Eqn. (3.4) shows that the observed data in l'-th coil can be obatained as the weighted sum of data from the other coils, where the weighting matrix used in Eqn. (3.4), is given as

$$\hat{\tilde{C}}_{l,l'} = \left(\sum_{l'' \neq l} \tilde{C}^H_{l'',l'} \tilde{C}_{l'',l'} \right)^{-1} \tilde{C}^H_{l,l'} \tag{3.5}$$

Now we divide the weighting matrix, $\hat{\tilde{C}}_{l,l'}$, of size $mN \times N^2$ in Eqn. (3.5) into M different Toeplitz matrices of size $mN \times mN$ along the column direction according to the relative locations in each block. The circulant elements in each resulting matrix is a vector of size mN, which, when reshaped back into a 2D matrix of size $m \times N$, yields a weighting map, $W_{s,l,l'} = \left(a_{s,l,l'}(k_x, k_y) \right)$, for the *l'*-coil that can be used to reconstruct data at a relative location, $s > 0$ (note that reconstructing data at $s = 0$ is redundant because those data have already been sampled) in each block. The missing data at a relative location, s, can then be reconstructed as

$$\begin{aligned} & d_{l'}(k_x, k_y + s\Delta k) \\ & \approx \sum_{l \neq l'} \sum_{k_x', k_y'} a_{s,l,l'}(k_x - k_x', k_y + s\Delta k - k_y') d_l(k_x', k_y'), \\ & \text{for } s = 1, 2, \cdots, M-1. \end{aligned} \tag{3.6}$$

This linear combination method follows the GRAPPA philosophy and is termed the extended GRAPPA algorithm.

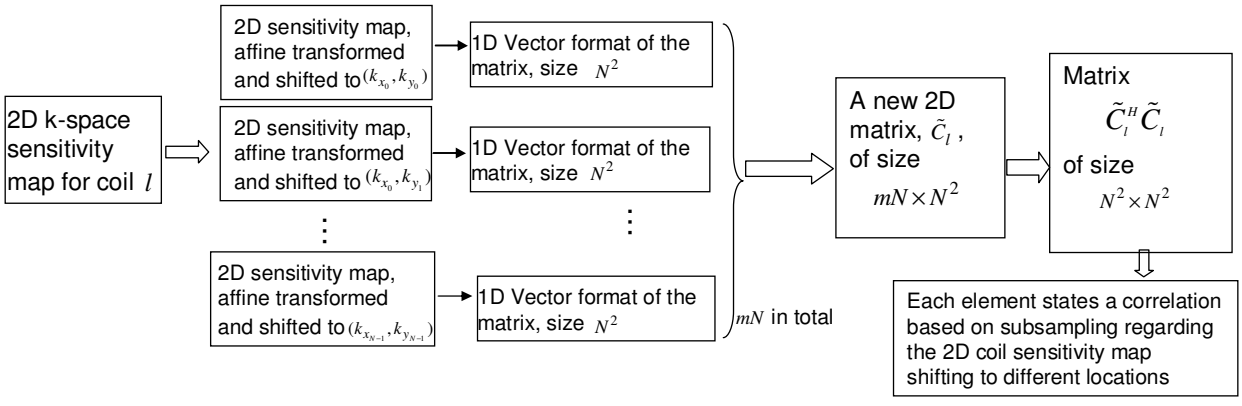

Fig. 1. Illustration of the matrix $\tilde{C}_l^H \tilde{C}_l$.

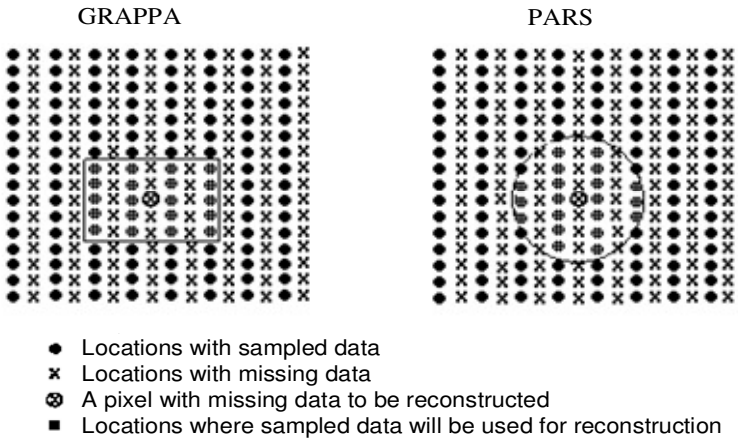

Fig. 2. Pixels used in GRAPPA reconstruction (left), inside a rectangle, length =7 pixels, width =5 pixels, compared to those pixels used in PARS reconstruction (right), inside a circle with radius=3.5 pixels.

4 The GRAPPA and PARS as the Approximation of GenSENSE

The proposed extended GRAPPA reconstruction method describes the weights for reconstructing each channel data in the same way as the GRAPPA algorithm. The only different is that the ratio of coil sensitivity maps is used for reconstructing data for each coil in the extended GRAPPA reconstruction.

In the extended GRAPPA algorithm, the weight maps for the relative location, s, in a block, are universal. They resemble the ratio of the *k*-space sensitivity maps with the most significant weights located in their central locations. In each *k*-space location where the missing data needed to be estimated, the weight maps are to be shifted to be centered upon the particular location as weights for reconstruction. This ensures the closer neighbors of the location have heavier weights used in the reconstruction. Therefore, optimal approximation can be constructed by choosing the most significant weights (in the center of the weight maps) while ignoring other small weights if we sort the weights according to their magnitude values, the same way as the SMASH algorithm. This is consistent with the GRAPPA and PARS methods where selected neighboring blocks and columns are involved in estimating the individual *k*-space coil data. Specially, we have the following relationship among the extended GRAPPA, GRAPPA, and PARS:

- Extended GRAPPA becomes the GRAPPA algorithm when a rectangle frame with R rows and P columns are involved in the reconstruction, see Fig. 2 (a),

$$d_{l'}(k_x, k_y + s\Delta k) \approx \sum_{l \neq l'} \sum_{k_y'=k_y-\frac{P}{2}}^{k_y+\frac{P}{2}-1} \sum_{k_x'=k_x-\frac{P}{2}}^{k_x+\frac{P}{2}-1} a_{s,l,l'}(k_x - k_x', k_y - k_y') d_l(k_x', k_y'), \quad (4.1)$$

for $s = 1,2,\cdots, M-1$

- Extended GRAPPA becomes the PARS algorithm when a circle frame radius r is involved in the reconstruction, namely

$$d_{l'}(k_x, k_y + s\Delta k) \approx \sum_{l \neq l'} \sum_{\left|(k_x', k_y') - (k_x, k_y + s\Delta k)\right| \le r} a_{s,l,l'}(k_x - k_x', k_y + s\Delta k - k_y') d_l(k_x', k_y'),$$

(4.2)

5 The Proposed Method

In this paper, using the theory developed in the previous sections 3 and 4, we proposed to extend the Eqn. (3.3) to the following

$$d_{l'}(k_x, k_y + s\Delta k) \approx \sum_{l \neq l'} \sum_{(k_x', k_y') \in G(k_x, k_y + s\Delta k)} a_{s,l,l'}(k_x - k_x', k_y + s\Delta k - k_y') d_l(k_x', k_y'),$$

(5.1)

where $G(k_x, k_y + s\Delta k)$ is a localized sub-region that is centered at a pixel $(k_X, k_Y + s\Delta k)$ in the *k*-space. This sub-region can be selected as a subset of the disk with a radius of r.

Further, it is interested to notice that an important feature with the usage of the auto-calibration signal (ACS) lines to determine the weights. The following explanation highlights the role of the ACS lines based on the proposed weight maps to be used for our algorithm. The connection between the data to be used and those from the ACS lines can be establish by rewriting Eqn. (5.1) as

$$d_{l'}\left(k_x, k_y + s\Delta k\right) = \sum_{l \neq l'} \sum_{\left(k_x', k_y'\right) \in R\left(k_x + s\Delta k, k_y\right)} a_{s,l,l'}\left(k_x', k_y'\right) d_l\left(k_x - k_x', k_y + s\Delta k - k_y'\right), \quad \text{for } s = 1,2,\cdots,M, \tag{5.2}$$

where $d_{l'}\left(k_x, k_y + s\Delta k\right)$ is the ACS data lines from the l'-th coil. Assume a is the amount of available ACS lines, for an approximation with degree, v, namely, v number of weights to be used in the approximation, and let $W_{l'}^{s}$ be the vector of the selected weights within a relative distance from a location, s where data are to be used in reconstruction using all the L' number participating coils. By integrating together the available data from the ACS lines of the l'-th coil into a vector $D_{s,l'}^{ACS}$, of size $u = Na$, we have

$$D_{ux1}^{ACS,,s} = \left(D_{u \times vL'}\right)\left(W_{l'}^{s}\right)_{vL' \times 1} \tag{5.3}$$

where D= $D_{u \times vL'}$ is the affine transformation of the data from other coils to be used as weights for reconstruction (according to Eqn. (5.3), and in the same formalism of Eqn. (5.1)). The weights can then be estimated as

$$W_{l'}^{s} = (D^H D)^{-1} D^H D_{s,l'}^{ACS}. \tag{5.4}$$

This equation demonstrates that the ACS lines essentially play the same role of providing the sensitivity information of the coils in determining the weights for reconstruction.

Using Eqn. (5.4), the number of weights used for reconstructing data from each coil can be decided by the ACS lines is limited by u / L'. Byond the limit, the solution will be ill-posted. In fact, the number of weights can be determined becomes much less when considering the correlations among the sub-sampled data. If only Eqn. (5.3) is used, this drawback becomes obvious when the number of weights needed to be estimated is increased. In the extreme case where the perfect reconstruction is pursued, it becomes obviously ill-posted where the number of weights needs to be decided is $\mathrm{L}' \times m \times \mathrm{N}$. Namely, the underestimation of weights would be a problem even using the full sampled data as ACS lines. This is because the matrix dimension of $D^H D$ is dramatically increased to $(m \times N \times L') \times (m \times N \times L')$. This reveals truth effect and limitation of the ACS lines on the reconstruction with the existing PARS algorithm.

Meanwhile, the ACS lines provide useful knowledge about the coil sensitivity. To retrieve the maximum information from the ACS lines, in this proposed method, we assume that Eqn. (5.4) is invariance with respect to the location, s. In the reverse direction, the ACS lines can be viewed as reconstructed from the sub-sampled data in its neighborhood, or the sub-sampled data can be viewed as reconstructed from the ACS lines; therefore, similar to Eqn. (5.4), another equation can be written by swapping the matrix D and W in Eqn. (5.4), which resulting in the following,

$$\left(D_{u',1}^{l'}\right) = D_{u'xvL'}^{ACS}\left(W_{l'}^{s}\right)_{vL' \times 1} \tag{5.5}$$

where $D_{u'xvL'}^{ACS}$ is the affine transform of the ACS lines from other coils to used as weights for reconstruction. Now, integrating together the Eqn. (5.4) and Eqn. (5.5) will result in a matrix of larger dimension as shown in the following equation,

$$\begin{pmatrix} D_{ux1}^{ACS,s} \\ D_{u'\times 1}^{l'} \end{pmatrix} = \begin{pmatrix} D_{u \times vL'} \\ D_{u' \times vL'}^{ACS} \end{pmatrix}\left(W_{l'}^{s}\right)_{vL' \times 1} \tag{5.6}$$

Now the left hand side is a vector of size $u + u'$. The weight matrix is then obtained as following

$$\left(W_{l'}^{s}\right)_{vL' \times 1} = \left(D_{u \times vL'}^{T}\left(D_{u'xvL'}^{ACS}\right)^{T} + D_{u \times vL'} D_{u'xvL'}^{ACS}\right)^{-1} \begin{pmatrix} D_{ux1}^{ACS,s} \\ D_{u'\times 1}^{l'} \end{pmatrix} \tag{5.7}$$

This results in using a matrix with increased rank in Eqn. (5.7) for calculating the weight coefficients to be used for reconstructing the full resolution image from the pMRI data. This improvement is new to the existing techniques, and we call this algorithm IPARS method. As shown in the experiment in the following section, this method dramatically increases the efficiency of using the information from the available data.

6 Simulation Studies

To demonstrate the advantage of our proposed IPARS reconstruction method, the algorithm was applied to simulated data using the Matlab software.

First, the simulation of the brain MRI image is obtained, and the sensitivity maps from eight receiver coils are simulated. The sensitivity maps are combined with the MRI to simulate the reduced sample MRI data from each channel. Specifically, a single-slice, sensitivity invariant MRI, of 64 x 64 points was simulated using the Brainweb simulated brain model (21), which was then combined with the simulated eight channel coil sensitivity maps to create 8 sets of sensitivity-variant MRI coil data of 64 x 64 points. The data were then Fourier transformed to *k*-space, from which the even samples in y-direction for each coil were selected to form 8 sub-sampled datasets of size 64 x 32. If zero filling is used for reconstruction, then the aliasing can be clearly observed, see Figure 1.

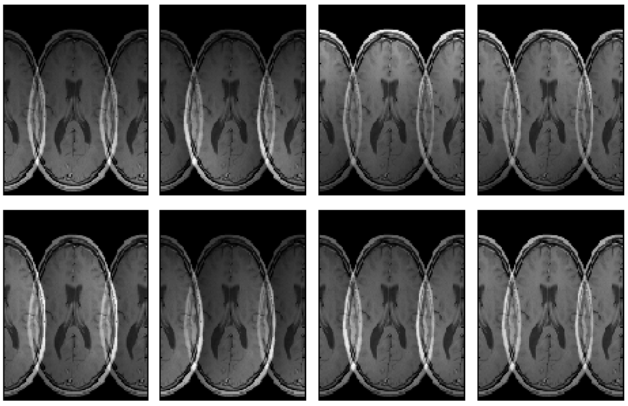

Figure 4. The 8 channel reconstructed images using zero filing method, with no ACS lines used.

Second, improved image reconstruction was run on the simulated data. In our reconstruction, one set of weight points focus in the center low frequency domain as shown in Figure 2 has been used to reconstruct the full resolution images. Namely, only those neighboring points around a pixel point is used for reconstruction.

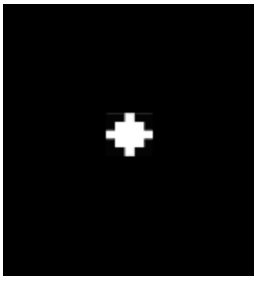

Figure 5. The set of weights used in reconstruction.

7 Results and Discussion

Shown in Figure 6(b) is the reconstructed image using our improved IPAR reconstruction method. IPAR has improved the PAR reconstruction and the usage of the ACS lines. The PAR reconstruction in Figure 6(a) used neighboring pixels data in each coils within a radius of 3 for reconstruction; the IPAR used 6 neighboring pixels for reconstruction. In both algorithms, three coils were involved in reconstructing the full resolution data in each coil. It is clearly shown that our improved algorithm reconstructed a full resolution image of high resolution and reduced aliasing. In contrast, the original PAR reconstruction has resulted in an image that, although in full resolution, some aliasing can still be observed clearly.

Our proposed reconstruction method alleviates the underweighted problems that most algorithms encountered, Only most significant weights are used for the reconstruction, and maximum information from ACS lines are used.

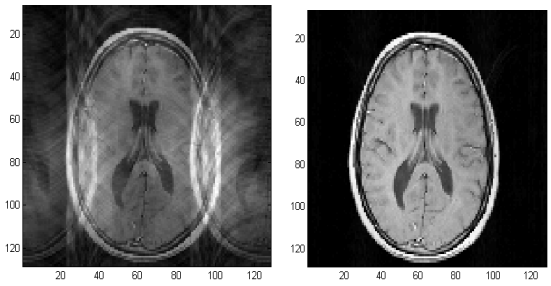

(a) (b)

Figure 6. The reconstruction results from (a) PAR reconstruction and (b) our proposed IPAR reconstruction.

8 CONCLUSION

In this paper, a mathematical understanding of the roles of the ACS lines has been presented to propose an improved reconstruction method IPAR base on the PARS algorithms so that the weight coefficients can be best determined for pMRI reconstruction.

9 Acknowledgement

The work in this paper was supported by the mini-grant of Faculty Summer Research Stipends, provided by the graduate school at Fayetteville State University.

10 References

[1] P. B. Roemer, *et al.*, "The NMR phased array," *Magnetic Resonance in Medicine,* vol. 16, pp. 192-225, 1990.

[2] K. P. Pruessmann, *et al.*, "SENSE: sensitivity encoding for fast MRI," *Magn Reson Med,* vol. 42, pp. 952-62, Nov 1999.

[3] J. B. Ra and C. Y. Rim, "Fast imaging using subencoding data sets from multiple detectors," *Magn Reson Med,* vol. 30, pp. 142-5, Jul 1993.

[4] W. E. Kyriakos, *et al.*, "Sensitivity profiles from an array of coils for encoding and reconstruction in parallel (SPACE RIP)," *Magn Reson Med,* vol. 44, pp. 301-8, Aug 2000.

[5] L. Ying, *et al.*, "On Tikhonov regularization for image reconstruction in parallel MRI," San Francisco, CA, 2004, pp. 1056-1059.

[6] F. H. Lin, *et al.*, "Parallel imaging reconstruction using automatic regularization," *Magn Reson Med,* vol. 51, pp. 559-67, Mar 2004.

[7] D. K. Sodickson and W. J. Manning, "Simultaneous acquisition of spatial harmonics (SMASH): fast imaging with radiofrequency coil arrays," *Magn Reson Med,* vol. 38, pp. 591-603, Oct 1997.

[8] M. A. Griswold, *et al.*, "Generalized autocalibrating partially parallel acquisitions (GRAPPA)," *Magn Reson Med,* vol. 47, pp. 1202-10, Jun 2002.

[9] Z. Wang, *et al.*, "Improved data reconstruction method for GRAPPA," *Magn Reson Med,* vol. 54, pp. 738-42, Sep 2005.

[10] E. N. Yeh, *et al.*, "Parallel magnetic resonance imaging with adaptive radius in k-space (PARS): constrained image reconstruction using k-space locality in radiofrequency coil encoded data," *Magn Reson Med,* vol. 53, pp. 1383-92, Jun 2005.

[11] A. A. Samsonov, *et al.*, "Advances in locally constrained k-space-based parallel MRI," *Magn Reson Med,* vol. 55, pp. 431-8, Feb 2006.

[12] K. P. Pruessmann, *et al.*, "Advances in sensitivity encoding with arbitrary k-space trajectories," *Magn Reson Med,* vol. 46, pp. 638-51, Oct 2001.

[13] K. P. Pruessmann, "Encoding and reconstruction in parallel MRI," *NMR Biomed,* vol. 19, pp. 288-99, May 2006.

[14] D. K. Sodickson, "A generalized basis approach to spatial encoding with coil arrays: SMASH-SENSE hybrids and improved parallel MRI at high accelerations," in *ISMRM*, ISMRM, Denver, 2000, p. 273.

[15] M. Blaimer, *et al.*, "SMASH, SENSE, PILS, GRAPPA: how to choose the optimal method," *Top Magn Reson Imaging,* vol. 15, pp. 223-36, Aug 2004.

[16] Y. Wang, "Description of parallel imaging in MRI using multiple coils," *Magn Reson Med,* vol. 44, pp. 495-9, Sep 2000.

[17] Y. Bao, " Mathematical Analysis of SMASH-Based Reconstruction Methods for Parallel MRI." *International Journal of Intelligent Computing in Medical Science and Image Processing, 4*(1), 65-76. 2011.

[18] W. S. Hoge, *et al.*, "A tour of accelerated parallel MR imaging from a linear systems perspective," *Concepts Magn Reson Part A,* vol. 27A, pp. 17-37, 2005.

[19] M. A. Griswold, *et al.*, "Parallel magnetic resonance imaging using the GRAPPA operator formalism," *Magn Reson Med,* vol. 54, pp. 1553-6, Dec 2005.

[20] M. Bydder, *et al.*, "Generalized SMASH imaging," *Magn Reson Med,* vol. 47, pp. 160-70, Jan 2002.

[21] Z.-P. Liang and P. C. Lauterbur, "A generalized series approach to MR spectroscopic imaging," *IEEE Transactions on Medical Imaging,* vol. 10, pp. 132-137, 1991 1991.

[22] http://www.bic.mni.mcgill.ca/brainweb/ [Online].

[23] Y. Bao, A. Maudsley Image Reconstruction in the Grappa Algorithm Formalism ISBI. 2007, pp.113-116.